Vol. 14 (2026): Proceedings of the 2nd International Conference on Artificial Intelligence, Modern Engineering and Environmental Sustainability (IC-AIMEES 2026)
E-ISSN: 3105-0522 P-ISSN：3105-0514
DOI: https://doi.org/10.70267/ ic-aimees.2026023240

Commonsense-Guided VLMs for 2D Fully Unobserved Object Detection

Ye Liu*

School of Artificial Intelligence, Shenyang University of Technology, Shenyang 110000, China

**Corresponding author: Ye Liu*

Abstract

This paper focuses on the task of 2D fully unobserved object detection, which requires inferring the presence and spatial distribution of targets that are entirely absent from the visible frame. Despite the potential of Vision-Language Models (VLMs), they often lack the spatial precision required for fine-grained 2D reasoning, while alternative diffusion-based methods incur prohibitive computational costs. To address these challenges, we propose CIUL, a novel reasoning framework that synergizes VLMs with structured prior knowledge through two core innovations: (1) Object-Oriented Commonsense Integration, which constructs an automated knowledge base to provide robust semantic constraints via typical spatial arrangements; and (2) Lightweight In-Context Learning, a paradigm that enables the model to adaptively refine its reasoning logic for unobserved regions using local visual cues from a single image without extensive retraining. Experimental results on the NYU Depth V2 benchmark demonstrate that our approach significantly out-performs existing baselines across key metrics, including 2D Region-wise Accuracy and Normalized Cross-Entropy, effectively bridging the gap between low-level perception and high-level commonsense reasoning.

Keywords

unobserved object detection, vision-language models, commonsense reasoning, in-context learning, spatial-semantic distribution

1. Introduction

In complex and dynamic real-world applications such as autonomous driving and intelligent robotics, environmental perception is the cornerstone of decision-making reliability and operational safety. Object detection, as acritical module within these systems, has achieved significant milestones in identifying and localizing entities within a camera's field of view. However, a fundamental gap remains: conventional systems are often "blind" to what lies just beyond the visible frame or behind opaque obstacles.

While a modal object detection and segmentation techniques [1] have partially addressed this by inferring the full shapes of partially occluded objects, they are inherently limited to cases where some visual evidence of the target is present. In practical scenarios—such as a pedestrian about to step out from behind a parked vehicle or furniture situated in a robot's camera blind spot—the target may be fully unobserved. As illustrated in Figure 1, using an indoor dining scene as an example, while the table and chair A are clearly visible, the

core challenge of 2D fully unobserved object detection is to precisely infer the presence and spatial distribution of chair B, which is entirely absent from the current image, based solely on observed contextual cues.

Figure 1: Illustration of the Unobserved Object Detection Task

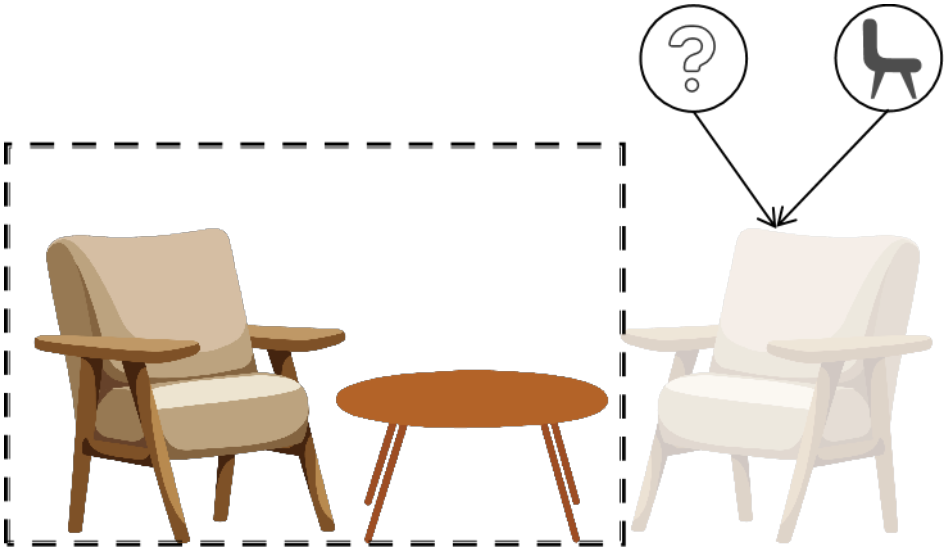

Despite its importance, current approaches to this reasoning task exhibit notable shortcomings. Vision-language models often lack the spatial preci- sion required to capture fine-grained positional relationships in 2D scenes, while diffusion-based generative models [2] incur prohibitive computational costs that hinder real-time deployment in robotics. Furthermore, existing studies rarely integrate object-level commonsense knowledge—such as the typical co-occurrence of furniture or traffic patterns—with contextual scene information, leading to a lack of effective prior constraints for reasoning about unobserved regions.

To address these challenges, we propose a novel framework that leverages the semantic reasoning strengths of VLMs while introducing structured prior constraints and efficient learning mechanisms. Specifically, we construct an automated commonsense knowledge base that translates typical spatial ar- rangements into concise textual prompts, providing the model with essential prior semantic constraints. Additionally, we design a lightweight in-context learning paradigm that enables the model to extract and utilize local visual cues from a single image to refine its reasoning logic for unobserved regions.

In summary, our contributions are:

• We propose the CIUL (Commonsense-enhanced In-context Unobserved Localizer) framework, which systematically leverages structured com- monsense information to enhance the spatial reasoning capabilities of VLMs for 2D fully unobserved object detection.

• We introduce a Lightweight In-Context Learning strategy that enables the model to utilize local visual context from a single image to adap- tively refine its reasoning logic for unobserved regions without the need for extensive retraining.

• Extensive experiments on the NYU Depth V2 dataset demonstrate the effectiveness of our proposed CIUL framework in achieving superior 2D distribution modeling and prediction accuracy compared to state- of-the-art methods.

The remainder of this paper is organized as follows: Section 2 discusses related work in spatial reasoning and unobserved detection; Section 3 details our proposed methodology; Section 4 presents experimental results and analysis; and Section 5 concludes the paper.

2. Related Work

The evolution of environment perception has moved from identifying visible entities to inferring unobserved spatial structures.Traditional object detection frameworks, ranging from CNN-based models like

Faster R-CNN [3] and YOLO [4] to Transformer-based architectures like DETR [5], pri- marily focus on identifying objects within the camera's direct line of sight.However, real-world complexity—characterized by frequent occlusions—has pushed the field toward amodal instance segmentation. Early works by Li and Malik [6] addressed the challenge of predicting the full extent of par- tially occluded objects. Subsequent improvements, such as the Hierarchical Occlusion Modeling in UOAIS-Net [7] and Bayesian generative approaches for out-of-distribution generalization [8], have significantly enhanced the recovery of occluded shapes. Despite these advances, amodal techniques remain fundamentally "observation-dependent," as they require at least a portion of the target to be visible to trigger the inference process.

The emergence of Vision-Language Models has shifted the focus from pure visual localization to cross-modal semantic reasoning. Models such as CLIP [9] and ALIGN [10] have demonstrated remarkable zero-shot capabilities by aligning visual features with textual descriptions. Nevertheless, their performance often degrades when faced with incomplete inputs or complex spatial compositions [11]. Recent benchmarks like CREPE [12] have highlighted that while VLMs possess vast world knowledge, they struggle to precisely capture atomic positional relationships in 2D scenes. This limitation suggests that relying solely on pre-trained visual-textual alignments is insufficient for rigorous spatial inference, necessitating the integration of structured prior knowledge to guide the reasoning process.

Bridging the gap between partial perception and global scene understanding, the task of fully unobserved object detection has recently been formalized. Unlike amodal detection, this task requires the model to infer objects that are entirely absent from the frame but exist in the immediate surroundings (e.g., blind spots). Bhattacharjee et al. [2] established the first standardized benchmark for this field, proposing a pipeline based on generative diffusion models and VLMs. While their work provides a foundational framework, the reliance on time-consuming diffusion processes and the lack of explicit commonsense constraints remain significant bottlenecks. Building upon this task definition, our work introduces an iterative optimization strategy that leverages object-level commonsense and in-context learning to achieve more accurate and efficient 2D spatial-semantic distribution modeling.

3. Method

This section details data process and detection pipelines based on a vision- language generative model, which estimates the 2D spatial-semantic distribution of targets from RGB images.

3.1 Data Process

3.1.1 Ground Truth Acquisition

To address the need for constructing 2D global probability distribution ground truth for semantic alignment tasks in vision-language models, this paper designs a ground truth extraction pipeline based on the YOLOv8x detection model. First, for input images with a fixed resolution of 360×640, a YOLO-compatible size is computed according to the 32× stride alignment rule to ensure completeness in detection feature extraction. After obtaining basic information such as bounding boxes and confidence scores through model inference, inverse sigmoid transformation is applied to approximate the object Logits and class Logits. The bounding boxes are then mapped from the YOLO-compatible size back to the original 360 ×640 resolution to maintain spatial coordinate consistency. Subsequently, detection results are grouped by semantic category to construct per-class spatial Logit mapping matrices. A maximum Logit filling strategy within bounding box regions is adopted to resolve semantic ambiguity in overlapping areas. After normalizing the Logit matrices via Softmax to obtain class probability distributions, the probability arrays are split into left/middle/right subregions in memory, concatenated, and processed through cropping/zero-padding operations, followed by global probability normalization, ultimately generating the required ground truth.

3.1.2 Input Processing

Vision-language models are adapted for predicting coarsely discretized 2D conditional distributions in this work. Before being input to the VLM, each 640×360 image is masked on both left and right sides with 140-pixel-wide black strips to simulate unobservable regions.

3.2 Pipeline

As shown in Figure 2, our proposed framework addresses the unobserved object detection task through a structured reasoning hierarchy. The pipeline synergizes visual perception with prior commonsense to infer objects beyond the camera's field of view

Figure 2: Overview of the proposed CIUL framework.

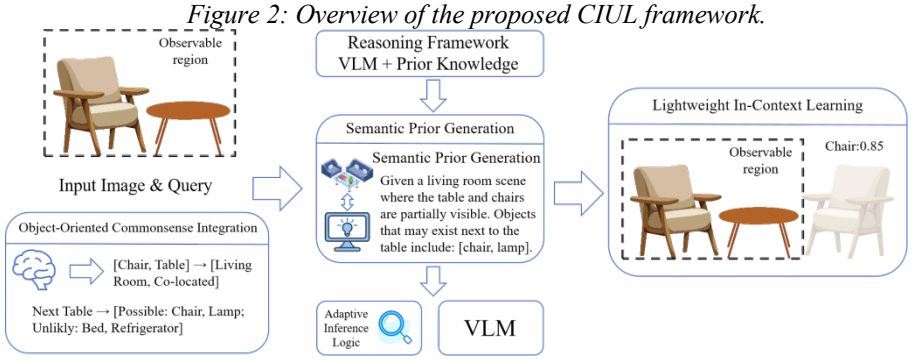

The pipeline synergizes visible images with structured commonsense priors (left), utilizing a Lightweight In-Context Learning engine to adaptively reason about unobserved areas (middle). This process generates precise 2D spatial distributions and probability maps for objects entirely absent from the visible frame (right).

3.2.1 Commonsense Knowledge Generation

To provide the model with essential prior constraints, we first develop an automated commonsense knowledge generation module. Given target categories identified by a preliminary detector, this module constructs structured prompts that encompass typical spatial arrangements, functional purposes, and co-occurrence patterns. Specifically, for each candidate category, the system prompts the vision-language model to generate a standardized knowledge base. This base serves as a semantic "anchor," translating abstract spatial relationships into actionable textual priors that guide the subsequent inference process for unobserved regions.

3.2.2 Semantic Description of Images

This stage complements global commonsense by focusing on extracting local visual cues from the 360×360 core frame. By integrating the previously generated commonsense priors into the reasoning loop, the VLM produces a fine-grained semantic description of the visible scene. This description goes beyond simple object recognition, capturing morphological attributes, spatial orientations, and interaction relationships among visible entities. This rich contextual representation provides the "evidence" for reasoning about objects that may exist in the adjacent black-masked regions.

3.2.3 Unobserved Object Detection

The final stage performs a probabilistic estimation of the 2D spatial- semantic distribution. Leveraging the synthesized knowledge from both global priors and local context, we implement a regional querying pipeline. For each target category and unobserved sub-region (Left/Right), the system submits structured "Yes/No" queries to the VLM. To ensure robust quantification, we employ an iterative sampling strategy (default: 10 queries per region). Confidence scores are derived from the frequency of positive responses and further refined via Softmax normalization, ultimately yielding the final 2D probability distribution.

3.3 Metrics for Unobserved Object Detection

To comprehensively evaluate the performance of the proposed method on the unobserved object detection task, this paper adopts the standardized evaluation metric system proposed by Bhattacharjee et al. [2], which includes Normalized Entropy (H), Normalized Cross-Entropy ($H^{\times}$), Normalized Nearest Neighbor Distance (Δ), False Negative Rate (FNR), and 2D Region-wise Accuracy (A). All metrics are computed based on the region- wise ground truth distribution (G_{I_0}) and the VLM-predicted distribution (D_{I_0}). This metric system effectively quantifies the alignment between the predicted and true distributions, spatial error, and classification accuracy, and is well-suited to the task characteristic of "true distribution being inaccessible" in unobserved object detection [2].

3.3.1 Normalized Entropy(*H*)

This metric quantifies the uncertainty of the predicted distribution, with normalization to constrain the result to the range $[0,1]$:

$$H = \frac{-\sum_{x \in X} D(x) \cdot \log(D(x))}{\log(|X|)} \tag{1}$$

where H represents the normalized entropy, $D(x)$ represents the predicted probability of region x, and $|X|$ represents the total number of discretized regions in the domain. The resulting values are clipped to $[0.0,1.0]$, where higher values indicate a more uniform predicted distribution and higher uncertainty.

3.3.2 Cross-Entropy($H^{\times}$)

To measure the alignment between the predicted and true distributions, normalized to eliminate the influence of region count:

$$H^{\times} = \frac{-\sum_{x \in X} G(x) \cdot \log(D(x))}{\log(|X|)} \tag{2}$$

where $H^{\times}$ represents the normalized cross-entropy, $G(x)$ represents the ground truth probability distribution for region x, $D(x)$ represents the predicted distribution, and $|X|$ represents the set of regions (typically $|X| = 3$ in this study). The resulting values are clipped to the range $[0.0, 2.0]$, where lower values indicate better alignment between the predicted and true distributions.

3.3.3 Normalized Nearest Neighbor Distance (Δ)

To measure the spatial deviation between the predicted peak and the true peak, the calculation steps are as follows:

$$dist(r_1, r_2) = \sqrt{(x_{r_1} - x_{r_2})^2 + (y_{r_1} - y_{r_2})^2} \tag{3}$$

where $dist(r_1, r_2)$ represents the Euclidean distance between two regions, (x_{r_1}, y_{r_1}) represents the center coordinates of the first region, and (x_{r_2}, y_{r_2}) represents the center coordinates of the second region. If there is no peak in either distribution, we set $\Delta = 1.0$; otherwise, the minimum distance is divided by the domain diameter and clipped to $[0.0,1.0]$.

3.3.4 False Negative Rate (FNR)

To measure the probability of the VLM missing target classes, a cumulative calculation is used:

$$FNR = \frac{\sum y(1 - \hat{y})}{\sum y} \tag{4}$$

where FNR represents the false negative rate, y represents the true label (where 1 indicates the region contains a target peak and 0 otherwise), and $\hat{y}$ represents the predicted label (where 1 indicates a predicted target peak and 0 otherwise). A lower value indicates a lower miss detection rate.

3.3.5 2D Region-wise Accuracy (A)

To measure the alignment between peak classification and true classes across 3 regions:

$$A = \frac{\sum_i [y_i = \hat{y}_i]}{l} \tag{5}$$

where A represents the 2D region-wise accuracy, l represents the number of sub-regions (set to 3 in this experiment), y_i represents the true label of the i-th region, $\hat{y}_i$ represents the predicted label of the *i*-th region, and $[y_i = \hat{y}_i]$ represents an indicator function that equals 1 when the labels match and 0 otherwise.

4. Experiments

4.1 Datasets and Evaluation Metrics

To validate the effectiveness of the proposed method for 2D unobserved object detection, we adopt the widely used NYU Depth V2 dataset [13] as the experimental benchmark, which is consistent with the setting of Bhattacharjee et al. [2]. This dataset focuses on indoor scenes (e.g., dining rooms, living rooms) and is well-suited for evaluating the ability to infer unobserved objects from partial visual cues. After automatic filtering based on object detection frequency [2], 10 representative scenes are selected for evaluation, with each scene containing an average of 1359 images. The original image resolution is 480×640, and two types of input images are used in experiments: the core input image I_0 (360×360, obtained by center cropping) and the expanded image I (360×640, generated by center cropping to match the 2D unobserved region extension task). For each scene, one frame is randomly selected as the input image I to ensure the generalization of evaluation results.

Object annotations for the expanded 360×640 image I are automatically generated by the YOLOv8x detector [26,53] pre-trained on the MS-COCO dataset [14], retaining only detections with confidence greater than $\tau_{conf} = 0.1$ [2]. The 2D ground-truth spatial distribution $G_{I_0}^{2D}$ is computed by softmax normalization of the detected object confidence logits. Note that only sceneobject pairs with non-empty ground-truth distributions are retained in the dataset to avoid invalid evaluations [2].

To comprehensively assess the performance of the proposed method, we employ the same set of 2D-specific evaluation metrics as Bhattacharjee et al.[2], which are specifically designed for the characteristics of 2D unobservedobject detection (e.g., multi-modality of true conditional distributions and inaccessibility of full realizations). The metrics include: (1) Normalized Entropy (*H*) [15], which quantifies the diversity of predicted 2D distributions and reflects the model's uncertainty about unobserved object locations, with a normalization factor $\log |X|$ (where X denotes the 2D discrete domain of 360×640 pixel grid) ensuring independence from grid resolution; (2) Normalized Cross-Entropy ($H^{\times}$), an asymmetric metric that measures the alignment between predicted and 2D ground-truth distributions, only penalizing low prediction probabilities where objects truly exist; (3) Normalized Nearest Neighbor Distance (Δ), which evaluates the spatial accuracy of predicted peaks by calculating the normalized distance between peaks of thresholded 2D ground-truth and prediction distributions; (4) False Negative Rate (FNR), which assesses the model's ability to avoid missing truly existing 2D unobserved objects; and (5) 2D Region-wise Accuracy (A), which measures the coarse-grained classification performance of determining object presence in three 2D sub-regions (360×360 core region, 360×140 left extended region, and 360×140 right extended region [2]). The classification threshold τ is set to $1.4/|X|$ [2], ensuring consistency with the original benchmark.

4.2 Implementation details

The hyperparameter settings are as follows: the classification threshold is set to $\tau = 1.4/|X|$, and the minimum detection confidence is $\tau_{conf} = 0.1$; for the region-wise accuracy calculation, the number of subregions $l = 3$ corresponds to the 360×360 input image region I, the 360×140 left-side region of the image, and the 360×140 right-side region of the image, respectively. For the vision-language models, we accessed Claude-Sonnet-4.5 via its official API. The temperature parameter was set to 0.25. The VLMs were queried 10 times per object, per region, and per scene.

4.3 Main Results

Table 1 presents a comprehensive quantitative comparison between our proposed framework and multiple state-of-the-art baselines on the NYU Depth V2 dataset-derived benchmark for unobserved object detection.

Our method achieves competitive performance across all primary evaluation metrics.he experimental results demonstrate that our method achieves competitive performance across all primary evaluation metrics, particularly in reducing missed detections while maintaining high classification accuracy.

Table 1: Quantitative evaluation of 2D fully unobserved object detection. We compare our method against baseline Vision-Language Models and traditional amodal reasoning approaches.

Method	H	$H^{\times}$	Δ	FNR	A
Uniform	1.000±0.000	1.000±0.000	∞	1.000	0.558±0.214
Oracle	0.714±0.143	0.714±0.143	0.000±0.000	0.000	1.000±0.000
Claude-4.5-Sonnet	0.961±0.190	1.120±0.605	0.801±0.348	0.445	0.981±0.090
CIUL(Ours)	**0.965±0.181**	**1.106±0.570**	**0.777±0.369**	**0.335**	**0.984±0.081**

Predictive Accuracy and Reliability. Our framework, which integrates com- monsense knowledge with Claude-4.5-Sonnet, achieves a 2D region-wise accuracy (A) of 0.984 ± 0.081, comparable to the VLM baseline (0.981). This indicates that while the classification task is relatively saturated for highperformance VLMs, our method effectively preserves the upper bound of recognition performance. More importantly, our approach significantly reduces the False Negative Rate (FNR) to 0.335, a marked improvement over the baseline (0.445). This 11% reduction suggests that integrating object-oriented commonsense knowledge and in-context learning effectively assists the model in "anticipating" objects entirely absent from the visual frame, thereby enhancing the reliability of the perception system in blind spots.

Distribution Alignment and Spatial Precision. Regarding distribution-based metrics, our method achieves a Normalized Cross-Entropy ($H^{\times}$) of 1.106 ± 0.570 and a Normalized Nearest Neighbor Distance (Δ) of 0.777 ± 0.369. These results outperform the VLM baseline ($H^{\times}$: 1.120, Δ: 0.801), indicating that the semantic priors generated by our framework provide stronger spatial constraints, leading to a more precise alignment between the predicted probability distributions and the actual ground truth.

Uncertainty and Calibration. The Normalized Entropy (H) for our method is 0.965, showing a slight increase compared to the baseline (0.961). This stability in entropy suggests that our model does not trade calibrated uncertainty for higher recall; instead, it maintains a cautious and reasonable decision boundary. Even when tasked with inferring unobserved regions, the framework avoids overconfident or hallucinatory assertions, demonstrating robust uncertainty estimation in challenging scenarios.

5. Conclusion

In this paper, we have proposed CIUL, a novel reasoning framework designed to address the challenging task of 2D fully unobserved object detection. By synergizing Vision-Language Models with Object-Oriented Commonsense Integration and a Lightweight In-Context Learning strategy, our approach effectively overcomes the limitations of existing methods in spatial precision and computational efficiency. Specifically, CIUL leverages structured prior knowledge to provide robust semantic constraints while adaptively refining reasoning logic using local visual cues from a single input image. Extensive evaluations on the NYU Depth V2 dataset demonstrate that our framework significantly enhances the accuracy of spatial distribution modeling and object localization. These results confirm the effectiveness of integrating commonsense reasoning into the perception pipeline, paving the way for more robust environment understanding in complex real-world scenarios

References

[1] Ling, H., Acuna, D., Kreis, K., Kim, S. W. and Fidler, S. Variational amodal object completion. In Advances in Neural Information Processing Systems 33 (NeurIPS 2020), San Diego, CA, USA, 2020, https://proceedings.neurips.cc/paper/2020/file/bacadc62d6e67d7897cef027fa2d416c-Paper.pdf.

[2] Bhattacharjee, S. S., Campbell, D. and Shome, R. Believing is Seeing: Unobserved Object Detection using Generative Models. In Proceedings of the IEEE/CVF Conference on Computer Vision and Pattern Recognition (CVPR), Music City Center, Nashville, Tennessee, USA, 2025; pp. 19366-19377. https://doi.org/10.1109/CVPR52734.2025.01804.

[3] Ren, S., He, K., Girshick, R. and Sun, J. Faster r-cnn: Towards real-time object detection with region proposal networks. Advances in neural information processing systems. 2015, pp. 91-99.

[4] Redmon, J., Divvala, S., Girshick, R. and Farhadi, A. You only look once: Unified, real-time object detection. In Proceedings of the IEEE conference on computer vision and pattern recognition, Las Vegas, Nevada, USA, 2016; pp. 779-788. https://doi.org/10.1109/CVPR.2016.91.

[5] Carion, N., Massa, F., Synnaeve, G., Usunier, N., Kirillov, A. and Zagoruyko, S. End-to-End Object Detection with Transformers. In Computer Vision - ECCV 2020. ECCV 2020, Cham, 2020; pp. 213-229. https://doi.org/10.1007/978-3-030-58452-8_13.

[6] Li, K. and Malik, J. Amodal Instance Segmentation. In Computer Vision – ECCV 2016. ECCV 2016, Cham, 2016; pp. 677-693. https://doi.org/10.1007/978-3-319-46475-6_42.

[7] Back, S., Lee, J., Kim, T., Noh, S., Kang, R., Bak, S. and Lee, K. Unseen Object Amodal Instance Segmentation via Hierarchical Occlusion Modeling. In 2022 International Conference on Robotics and Automation (ICRA), Philadelphia, PA, USA, 2022; pp. 5085-5092. https://doi.org/10.1109/ICRA46639.2022.9811646.

[8] Sun, Y., Kortylewski, A. and Yuille, A. Amodal segmentation through out-of-task and out-of-distribution generalization with a bayesian model. In Proceedings of the IEEE/CVF conference on computer vision and pattern recognition, Piscataway, NJ, USA, 2022; pp. 1215-1224. https://doi.org/10.1109/CVPR52688.2022.00128.

[9] Radford, A., Kim, J. W., Hallacy, C., Ramesh, A., Goh, G., Agarwal, S., Sastry, G., Askell, A., Mishkin, P. and Clark, J. Learning transferable visual models from natural language supervision. In International conference on machine learning, London, UK, 2021; pp. 8748-8763, http://proceedings.mlr.press/v139/radford21a.html.

[10] Jia, C., Yang, Y., Xia, Y., Chen, Y.-T., Parekh, Z., Pham, H., Le, Q., Sung, Y.-H., Li, Z. and Duerig, T. Scaling up visual and vision-language representation learning with noisy text supervision. In International conference on machine learning, London, UK, 2021; pp. 4904-4916, http://proceedings.mlr.press/v139/jia21b.html.

[11] Chen, B., Xu, Z., Kirmani, S., Ichter, B., Sadigh, D., Guibas, L. and Xia, F. Spatialvlm: Endowing vision-language models with spatial reasoning capabilities. In Proceedings of the IEEE/CVF Conference on Computer Vision and Pattern Recognition, Seattle, Washington, USA, 2024; pp. 14455-14465, https://openaccess.thecvf.com/content/CVPR2024/papers/Chen_SpatialVLM_Endowing_Vision-Language_Models_with_Spatial_Reasoning_Capabilities_CVPR_2024_paper.pdf.

[12] Thrush, T., Jiang, R., Bartolo, M., Singh, A., Williams, A., Kiela, D. and Ross, C. Winoground: Probing vision and language models for visio-linguistic compositionality. In Proceedings of the IEEE/CVF Conference on Computer Vision and Pattern Recognition, Piscataway, NJ, 2022; pp. 5238-5248. https://doi.org/10.1109/CVPR52688.2022.00517.

[13] Silberman, N., Hoiem, D., Kohli, P. and Fergus, R. Indoor Segmentation and Support Inference from RGBD Images. In Computer Vision – ECCV 2012. ECCV 2012. Lecture Notes in Computer Science, Berlin, Heidelberg, 2012; pp. 746-760. https://doi.org/10.1007/978-3-642-33715-4_54.

[14] Lin, T.-Y., Maire, M., Belongie, S., Hays, J., Perona, P., Ramanan, D., Dollár, P. and Zitnick, C. L. Microsoft COCO: Common Objects in Context. In Computer Vision – ECCV 2014. ECCV 2014. Lecture Notes in Computer Science, Cham, 2014; pp. 740-755.

[15] Shannon, C. E. A mathematical theory of communication. SIGMOBILE Mobile Computing and Communications Review. 2001, 5(1), pp. 3–55. https://doi.org/10.1145/584091.584093.

Funding

This research received no external funding.

Conflicts of Interest

The authors declare no conflict of interest.

Acknowledgment

This paper is an output of the science project.